

See discussions, stats, and author profiles for this publication at: <https://www.researchgate.net/publication/228492801>

# Effects of Structural Differences on Metallic Corrosion Inhibition by Metal–Polyphosphonate Thin Films

ARTICLE *in* INDUSTRIAL & ENGINEERING CHEMISTRY RESEARCH · NOVEMBER 2006

Impact Factor: 2.59 · DOI: 10.1021/ie0607898

---

CITATIONS

35

---

READS

114

3 AUTHORS, INCLUDING:



[Konstantinos D Demadis](#)

University of Crete

142 PUBLICATIONS 3,654 CITATIONS

SEE PROFILE

# Effects of Structural Differences on Metallic Corrosion Inhibition by Metal–Polyphosphonate Thin Films

Konstantinos D. Demadis,\* Chris Mantzaridis, and Panagiotis Lykoudis

Crystal Engineering, Growth and Design Laboratory, Department of Chemistry, University of Crete, P.O. Box 2208, Voutes Campus, Heraklion, Crete, GR-71003, Greece

A series of metal–phosphonate organic–inorganic polymeric hybrid materials are synthesized, structurally characterized, and evaluated for their anticorrosion properties for the protection of carbon steels. These materials are Zn–AMP (where AMP = amino-tris(methylenephosphonate)), Zn–HDTMP (where HDTMP = hexamethylenediamine-tetrakis(methylenephosphonate)), and Ca–PBTC (where PBTC = 2-phosphonobutane-1,2,4-tricarboxylate)). Their structures are described and compared. Their corrosion inhibition performances are also compared, and some interesting conclusions are drawn that relate molecular structure to inhibitory activity.

## Introduction

Corrosion has been defined in many ways. The definitions, although different in expression, have all emphasized the changing of the mechanical properties of metals in an undesirable way. ISO 8044 defines corrosion as “physicochemical interaction, which is usually of an electrochemical nature, between a metal and its environment results in changes in the properties of the metal and which may often lead to impairment of the function of the metal, the environment, or the technical system of which these form a part”.<sup>1</sup> The cost of corrosion has been reported from many studies to be on the order of 1%–5% of the gross national product for any country. Worldwide, the cost of corrosion for the production of all grades of pulp is approximately \$3 billion/year. These numbers do not include the cost of lost production, shutdowns to make repairs to corroded equipment, etc. Corrosion costs in the United States electric power industry reaches \$10 billion each year, according to the Electric Power Research Institute (EPRI). Also, EPRI has reported that corrosion is the cause of more than 55% of all unplanned outages, and it adds over 10% to the average annual household electricity bill. The impact of corrosion on all branches of industry in almost all countries can be observed. For example, in 1993, it was estimated that 60% of all maintenance costs for North Sea oil production platforms were related to corrosion, either directly or indirectly. A report on inspection results of several offshore production plants showed that corrosion was a factor in 35% of the structures, 33% of the process systems, and 25% of the pipelines. Corrosion management can be achieved in several ways, one of which is based on corrosion inhibitors. These are chemical additives that delay or (ideally) stop metallic corrosion.<sup>2</sup>

Corrosion inhibitors are effective for the decrease of metal corrosion under almost-neutral conditions by forming sparingly soluble compounds with the metal ion existing in the solution, which precipitate onto the surface to form a thin protective layer. Such inhibitors (which are often called interphase inhibitors) for cooling-water treatment technology in the past decades integrate different types of phosphonates.<sup>3</sup> Widely used examples of organic phosphonates include 1-hydroxyethane-1,1-

diphosphonic acid (HEDP), amino-tris(methylenephosphonic acid) (AMP), and hydroxyphosphonoacetic acid (HPA). Phosphonates are introduced into the system to be protected in the acid form or as alkali-metal soluble salts, but readily form more stable complexes with other metal cations found in the process stream (most commonly, Ca, Mg, Sr, or Ba), depending on the particular application. Research in this area has been stimulated by the need to develop inhibitor formulations that are free of chromates, nitrates, nitrites, inorganic phosphorus compounds, etc. Phosphonates, when blended with certain metal cations and polymers, reduce the optimal inhibitor concentration needed for inhibition due to synergistic effects.<sup>4</sup> Synergism is one of the important effects in the inhibition process and serves as the basis for the development of all modern corrosion inhibitor formulations.

Despite the significant body of literature, evidence about the molecular identity of the thin protective metal phosphonate films lags behind. In this paper, we report the corrosion inhibition performance of three metal phosphonate materials that exhibit dramatically different anticorrosion efficiencies, which are linked to their molecular structure. These are Zn–AMP ( $\{Zn[(HO_3PCH_2)_3N(H)] \cdot 3H_2O\}_n$ ), Zn–HDTMP ( $\{Zn[(HO_3PCH_2)_2N(H)(CH_2)_6N(H)(CH_2PO_3H)_2] \cdot H_2O\}_n$ ), and Ca–PBTC ( $\{Ca(HOOC-CH_2C(COO)(PO_3H)CH_2CH_2COOH)(H_2O)_2 \cdot 2H_2O\}_n$ ).

## Experimental Section

**Metal Phosphonate Materials: Synthesis and Characterization.** All chemicals were obtained from commercial sources. The additives used in this study are shown schematically in Figure 1. The syntheses of these materials are reported elsewhere.<sup>5–7</sup> Preliminary structural data have been reported previously. Crystallographic data for the structures discussed herein have been deposited with the Cambridge Crystallographic Data Centre (CCDC Nos. 257224 (Zn–AMP), 258076 (Zn–HDTMP), and 258096 (Ca–PBTC)). [Copies of the data may be obtained free of charge from the Director, Cambridge Crystallographic Data Centre, 12 Union Road, Cambridge, CB2 1EZ, U.K.; fax, +44-1223-336033; e-mail: deposit@ccdc.cam.ac.uk; URL: <http://www.ccdc.cam.ac.uk>.]

**Corrosion Inhibition Protocol.** Corrosion specimens (carbon steel C1010) are prepared according to established protocols.<sup>8</sup> Each coupon is immersed in a control solution (no inhibitor) or in a test solution (1.0 mM  $Zn^{2+}$  and 1.0 mM AMP) at pH

\* To whom correspondence should be addressed. Tel.: +30-2810-545051. Fax: +30-2810-545001. E-mail address: demadis@chemistry.uoc.gr. URL: <http://www.chemistry.uoc.gr/demadis>.

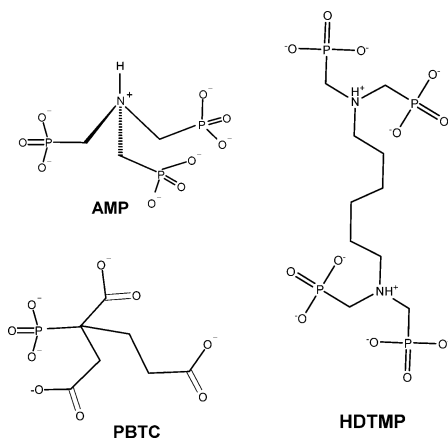


**Figure 1.** Schematic structures of the AMP, HDTMP, and PBTC corrosion inhibitors.

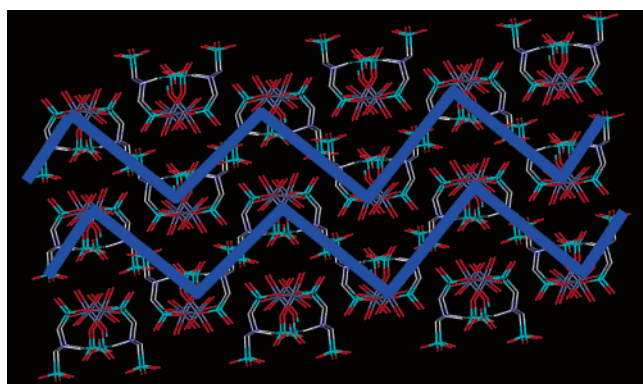


**Figure 2.** Zigzag chains in the crystal structure of Zn-AMP. The “corners” are the Zn centers, and the linear parts of the chain are the uncomplexed phosphonate group.

3.0, and the progress of corrosion is monitored by visual inspection for three days. The specimens then are removed from solution, surface samples are taken for spectroscopic studies, and corrosion products are cleaned by a standard method to determine corrosion rates from mass loss. Note that these conditions are purposely exaggerated, compared to those found in actual field applications. The same protocol was used for Zn-HDTMP (at pH 2.2), for Ca-PBTC (at pH 4.0) and for Zn-PBTC (at pH 4.0).

## Results

**Crystal Structures of Metal Phosphonates.** In the structure of Zn-AMP, AMP maintains its “zwitterion” character in the crystal lattice because each phosphonate group is singly deprotonated, whereas the N atom is protonated. The  $\text{Zn}^{2+}$  cation is coordinated by three phosphonate oxygens and three  $\text{H}_2\text{O}$  molecules. AMP forms an eight-membered chelate ring with the  $\text{Zn}^{2+}$  cation. The bond angles indicate a slightly distorted octahedral geometry, with the largest deviation being  $166.90(6)^\circ$ . The third phosphonate arm, surprisingly, is *not* coordinated to the  $\text{Zn}^{2+}$  cation, but is exclusively involved in hydrogen bonding. A zigzag chain parallel to the *c*-axis is formed by the  $\text{Zn}^{2+}$  cation (see Figure 2). The  $\text{Zn}^{2+}$  centers are located at the corners of the zigzag chain, whereas the “linear” portion of the zigzag is made of the noncoordinated, hydrogen-bonded phosphonate groups. The presence of a noncoordinated, singly deprotonated phosphonate group in the lattice is somewhat surprising. This phosphonate moiety participates in a complicated hydrogen bonding network that presumably “relieves” the presence of the negative charge.

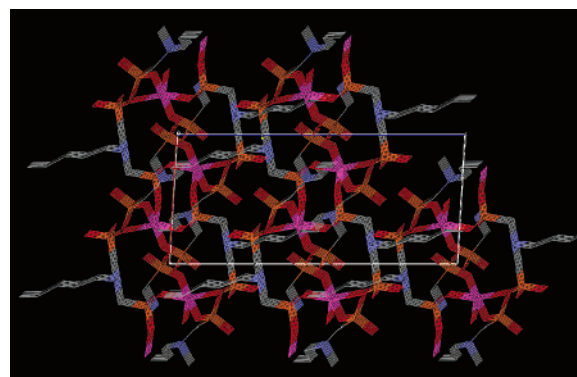


**Figure 3.** Crystal lattice of Zn-HDTMP, viewed parallel to the *b*-axis. Color code: Zn (purple), C (gray), P (orange), N (blue), and O (red).

The crystal structure of Zn-HDTMP shows that it is a three-dimensional (3D) coordination polymer (see Figure 3). The Zn-O distances are unexceptional and consistent with other structurally characterized zinc-phosphonates.<sup>9–14</sup> The  $\text{Zn}^{2+}$  cation is found in a distorted octahedral environment that is formed exclusively by phosphonate oxygens.

The  $\text{C}_6$  carbon chain runs almost parallel to the *bc* diagonal. Also, it does not possess the expected zigzag configuration; however, the portion  $\text{C}(2)\text{--}\text{C}(3)\text{--}\text{C}(5)\text{--}\text{C}(6)$  is in a “syn” rather than “anti” configuration.

The crystal structure of Ca-PBTC reveals a polymeric material with PBTC acting as a tetradentate chelate. The  $\text{Ca}^{2+}$  center is seven-coordinated in a capped octahedral environment, bound by two phosphonate oxygens, three carboxylate oxygens, and two water molecules. The phosphonate oxygens act as bridges between two neighboring Ca centers, located  $6.781 \text{ \AA}$  apart. All three carboxylate oxygens are protonated. The protonated  $\text{--COOH}$  group is coordinated to the Ca through the carbonyl atom. This is consistent with the long  $\text{Ca--O(=C)}$  distances of  $2.470(2)$  and  $2.448(2) \text{ \AA}$ . Such  $\text{Ca--O=C(OH)}$  coordination modes are rare.<sup>15,16</sup> The bridging  $\text{--PO}_3^{2-}$  tetrahedra and the  $\text{CaO}_7$  polyhedra are arranged in a zigzag chain configuration that is oriented parallel to the *b*-axis. This is depicted in Figure 4.

Both *R* and *S* stereoisomers (according to the Cahn-Ingold-Prelog sequence) of PBTC are present in the structure of  $\text{Ca(PBTC)(H}_2\text{O)}_2 \cdot 2\text{H}_2\text{O}$  in a regular pattern. Each chain shown in Figure 4 contains only one PBTC stereoisomer.

**Metallic Corrosion Inhibition by Metal Phosphonate Thin Films.** Synergistic combinations of a 1:1 molar ratio of  $\text{Zn}^{2+}$  and AMP are reported to exhibit superior inhibition performance than either  $\text{Zn}^{2+}$  or AMP alone.<sup>17–19</sup> However, no mention is made regarding the identity of the inhibitor species involved in corrosion inhibition. Therefore, a corrosion experiment is designed to verify the literature results and prove that the protective material acting as a corrosion barrier is an organic-inorganic hybrid composed of Zn and AMP. A synergistic combination of  $\text{Zn}^{2+}$  and AMP in a 1:1 ratio (under identical conditions used to prepare crystalline Zn-AMP) offers excellent corrosion protection for carbon steel (see Figure 5).

Although differentiation between the “control” and “Zn-AMP” protected specimens is evident within the first hours, the corrosion experiment is allowed to proceed over a three-day period. Based on mass loss measurements, the corrosion rate for the “control” sample is  $2.5 \text{ mm/yr}$ , whereas for the Zn-AMP protected sample  $0.9 \text{ mm/yr}$ , which is a 270% reduction in the corrosion rate. The filming material is collected and subjected to Fourier transform infrared (FT-IR) spectroscopy, X-ray fluorescence (XRF), and energy-dispersive spectroscopy

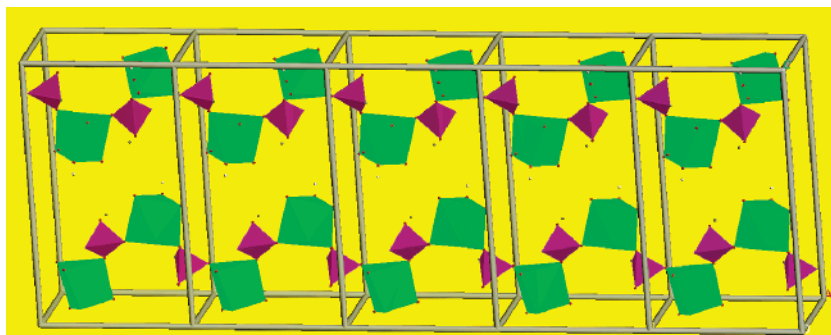


**Figure 4.** View of two zigzag chains over five unit cells formed by  $\text{CaO}_7$  polyhedra (green) and  $\text{PO}_3\text{C}$  tetrahedra (magenta) that are oriented parallel to the *b*-axis.

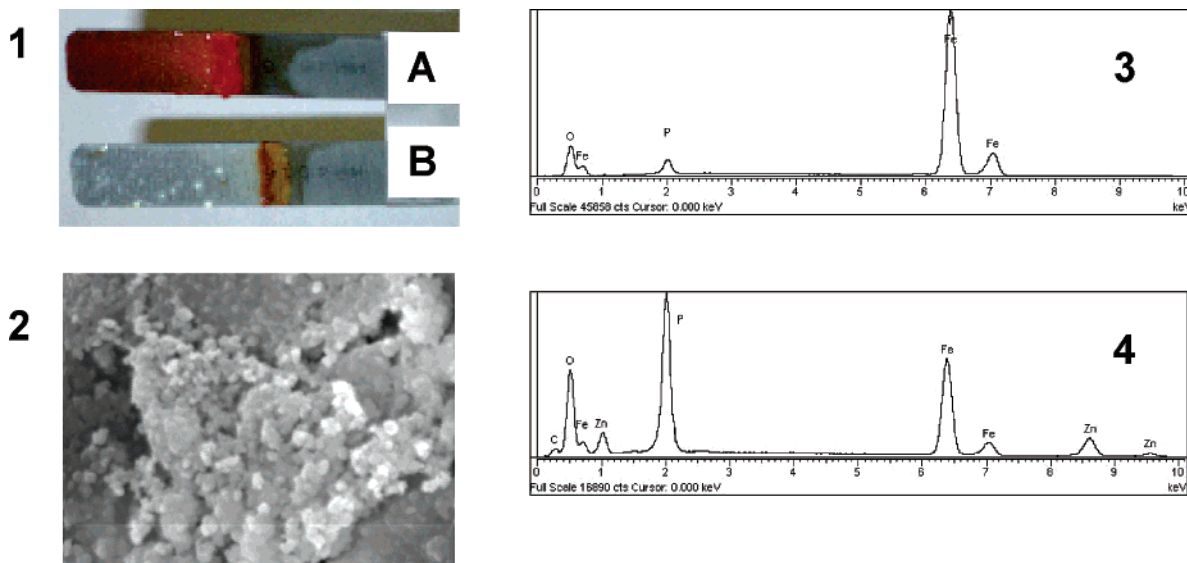


**Figure 5.** Panel 1: corrosion inhibition by Zn-AMP. The upper specimen (A) is the control, no inhibitor present; the lower specimen (B) is with a  $\text{Zn}^{2+}$ /AMP combination present, both in 1 mM. Corrosion inhibition is dramatically demonstrated at pH 3.0. The formation of Zn-AMP can be clearly seen on the steel specimen as a thin white layer, with additional material accumulated at certain locations, appearing as white spots. Panel 2: surface texture of the inhibiting Zn-AMP film (bar = 8  $\mu\text{m}$ ). EDS results are also given, showing an absence of Zn/P on an unprotected surface (panel 3) and their presence on a protected surface (panel 4).

(EDS) studies. These show that the inhibiting film is a material that contains zinc (from added  $\text{Zn}^{2+}$ ) and phosphorus (from added AMP) in an  $\sim 1:3$  ratio, as expected. Iron was also present, which apparently originated from the steel specimen. FT-IR spectroscopy showed multiple bands that were associated with the phosphonate groups that closely resemble those of an authentically prepared Zn-AMP material. For comparison, EDS and XRF spectra of a “protected” and an “unprotected” region show the presence of zinc and phosphorus in the former, but a complete absence of both in the latter.

A combination of  $\text{Zn}^{2+}$  and HDTMP in a 1:1 ratio (under conditions identical to those used to prepare crystalline Zn-HDTMP) offers excellent corrosion protection for carbon steel (see Figure 6). Although differentiation between the “control” and “Zn-HDTMP”-protected specimens is profound within the first hours, the corrosion experiment is allowed to proceed over a three-day period. Based on mass loss measurements, the corrosion rate for the “control” sample is 7.28 mm/yr, whereas for the Zn-HDTMP protected sample, the corrosion rate is 2.11 mm/yr, which is an  $\sim 170\%$  reduction in the corrosion rate. The filming material is collected and subjected to FT-IR, XRF, and EDS studies. These analyses show that the corrosion-inhibiting film is a material that contains  $\text{Zn}^{2+}$  (from externally added  $\text{Zn}^{2+}$ ) and phosphorus (from added HDTMP) in an  $\sim 1:4$  ratio. Iron was also present, which apparently originated from the carbon steel specimen. FT-IR spectroscopy of the filming

material showed multiple bands that were associated with the phosphonate groups in the 950–1200  $\text{cm}^{-1}$  region that closely resemble those of the authentically prepared Zn-HDTMP material (see Figure 6). For comparison, EDS and XRF spectra of a “protected” and an “unprotected” region indicate the presence of zinc and phosphorus in the former, but a complete absence of both in the latter.

A synergistic combination of  $\text{Ca}^{2+}$  and PBTC in a 1:1 molar ratio (under conditions identical to those used to prepare crystalline  $\text{Ca}(\text{PBTC})(\text{H}_2\text{O})_2 \cdot 2\text{H}_2\text{O}$ ) seems to offer excellent corrosion protection for carbon steel (see Figure 7), based on visual observations. However, based on mass loss measurements,<sup>8</sup> the corrosion rate for the “control” sample is 0.16 mm/yr, whereas for the Ca-PBTC protected sample, the corrosion rate is 1.17 mm/yr, which is an  $\sim 10$ -fold increase in the corrosion rate. Therefore, PBTC essentially enhances the dissolution of bare metal, presumably forming soluble Fe-PBTC complexes. In contrast to aminomethylene-tris-phosphonate (AMP), PBTC does not form stable metal phosphonate protective films. This is consistent with the low complex formation constant for Ca-PBTC (4.4).<sup>20</sup>

## Discussion

Phosphonates are better known for their antiscaling/antifouling properties,<sup>21</sup> rather than their anticorrosion efficiency.



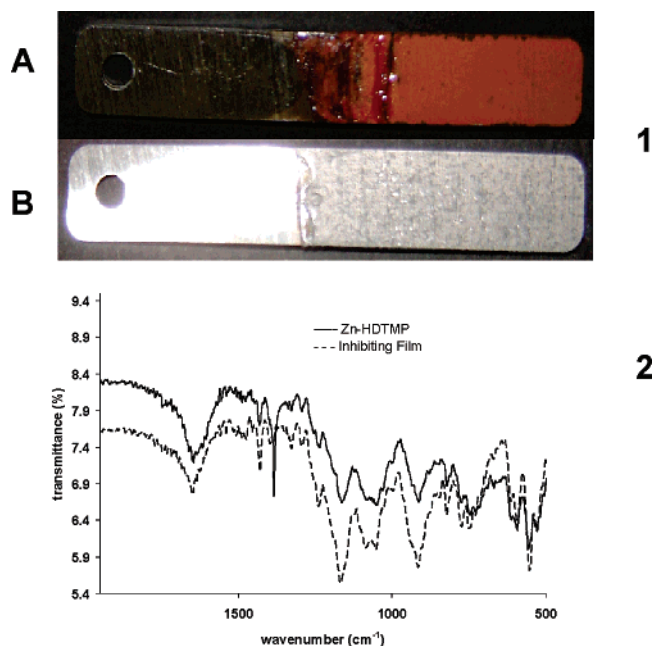


**Figure 6.** Anticorrosive effect of Zn-HDTMP films on carbon steel. Panel 1 shows that the upper specimen is the “control” (A), with no inhibitor present; corrosion inhibition in the lower specimen (B) by a 1 mM  $\text{Zn}^{2+}$ /HDTMP synergistic combination is dramatically demonstrated. Panel 2 shows FT-IR spectra of “genuine” Zn-HDTMP and the protective film.



**Figure 7.** Phenomenology of the anticorrosive effect of Ca-PBTC films on carbon steel. The upper specimen is the “control” (A), with no inhibitor present. Surface “cleanliness” in the lower specimen (B) by a 1 mM  $\text{Ca}^{2+}$ /PBTC synergistic combination is demonstrated, but metal loss is enhanced (see text).

However, the latter can be substantially improved in the presence of metal ions. This synergistic phenomenon has been extensively and elegantly studied, primarily by electrochemical methods.<sup>22,23</sup> Notably, the work of Telegdi et al. has given insight into the possible mechanism of corrosion protection.<sup>24</sup> Kuznetsov has extensively and systematically studied a variety of inhibitors that have complexing properties.<sup>25</sup>

An ideal phosphonate corrosion inhibitor of the “complexing type” is required to possess the following significant features: (a) it must be capable of generating metal phosphonate thin films on the surface to be protected; (b) it should not form very soluble metal complexes, because these will not eventually “deposit” onto the metal surface, but, instead, will remain soluble in the bulk; (c) it should not form sparingly soluble metal complexes, because these may never reach the metal surface to achieve inhibition, but may generate undesirable deposits in the bulk or on other critical system surfaces; and (d) its metal complexes that are generated by controlled deposition on the metal surface must create dense thin films with robust structure thus preventing oxygen diffusion through the film and towards the metal surface. If the anticorrosion film is nonuniform or porous, then uneven

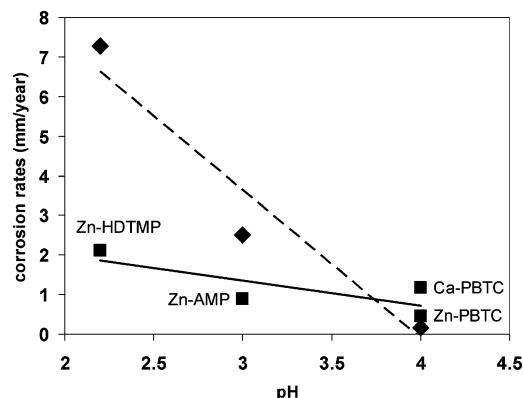


**Figure 8.** Corrosion rates of metal-phosphonate-protected surfaces, as a function of pH. Rhombs represent the “control” for pH and squares represent the individual inhibitors, as shown.

oxygen permeation may create sites for localized attack, leading to pitting of the metal surface.

The present study described herein is more geared toward understanding corrosion inhibition at the molecular level, rather than proving the anticorrosion performance of the aforementioned inhibitors. There are several hypotheses found in the literature on the mechanism of corrosion inhibition by metal-inhibitor complexes and are supported by a variety of spectroscopic and electrochemical techniques. However, none of these has unequivocally proven the molecular identity of the metal-inhibitor complex.

The corrosion inhibition results are presented in Figure 8. It is apparent that pH has a profound role in corrosion inhibition. A decrease of 2 pH units causes a 45-fold increase in the corrosion rate and operational range (from 0.16 mm/yr to 7.28 mm/yr).

This is consistent with well-established observations in laboratory experiments and in real water systems in the field. The presence of a metal phosphonates causes a dramatic decrease in the overall corrosion rates. Again, lower operational pH favors higher corrosion rates; however, the operational range is now much narrower (from 0.90 to 2.11 mm/yr). This translates to an ability to operate with lower-pH process waters with acceptable corrosion rates; however, the presence of a metal phosphonate corrosion inhibitor is necessary. The results with Ca-PBTC and Zn-PBTC warrant further discussion. Corrosion rates in the presence of an inhibitor are greater than those for the control (with no inhibitor). This, at first glance, is contrary to the results obtained with the Zn-HDTMP and Zn-AMP inhibitors. This may be explained by several arguments. First, the metal-phosphonate film may not be robust but porous in its microscopic nature. This, as mentioned previously, would lead to localized attack and metal pitting. Such phenomena have not been observed upon examination of the metal specimens after the corrosion experiments. Second, the metal phosphonate (Ca-PBTC or Zn-PBTC) is too soluble to deposit onto the metal surface; therefore, it does not form a protective and anticorrosion thin film. Although this argument is a logical assumption at this point, based on available literature data,<sup>20</sup> more experiments must be conducted to confirm it experimentally. These are underway in our laboratory. However, this argument would be consistent with literature data on metal-PBTC complex formation constants (4.4 for Ca-PBTC and 8.3 for Zn-PBTC), which are considered to be very low.<sup>20</sup> The difference in complex formation constants between Ca-PBTC and Zn-PBTC would be consistent with the fact that Zn-PBTC is a more effective corrosion inhibitor than Ca-PBTC, as long

as both inhibitors form films (albeit unstable) on the metal surface. If film formation does not occur, then corrosion rates in the presence of Ca–PBTC or Zn–PBTC would be the same as the control, which is not the case.

Therefore, the results obtained with Ca–PBTC and Zn–PBTC indicate that these materials are soluble and, because of their acidic nature (PBTC in Ca–PBTC has three dissociable protons), they actually act as metal dissolvers rather than corrosion inhibitors. A careful look at the molecular structure of Ca–PBTC reveals that PBTC is doubly deprotonated (at the phosphonate group and at the carboxyl group at the 6 position). The remaining two carboxylate groups are protonated but coordinated to the  $\text{Ca}^{2+}$  center through the  $\text{C}=\text{O}$  moiety. This increases the acidity of the noncoordinated  $-\text{OH}$  group of the carboxylate. The final result could be considered to be the formation of a Ca–PBTC soluble acidic complex at the proximity or on the metal surface, which acts as an iron oxide dissolver. Alternatively, this acidic complex may create local low-pH regions, which would certainly increase corrosion rates.

The two zinc–phosphonates have distinctly different crystal and molecular structures. The Zn–HDTMP material, by virtue of its long chain linker between the two amino-bis(methylene-phosphonate) moieties, might be considered to be a porous material. However, porosity measurements on this and the other phosphonates show an absence of any porous structure. Therefore, differences in porosity cannot be invoked to explain the anticorrosion performance variability of these metal–phosphonate materials.

Lastly, the ability of a metal–phosphonate corrosion inhibitor to adhere onto the metal surface plays a vital role in corrosion efficacy. Bulk precipitation of a metal–phosphonate complex will lead to a loss of active inhibitor to precipitation, leading to insufficient levels for thin-film formation. Surface adherence of the inhibitor films is a property that cannot be precisely predicted. However, it is a necessary condition for acceptable inhibition. In addition, the metal–phosphonate protective layer must be robust and uniform. A characteristic example of a Zn–AMP film is shown in Figure 9 and is compared to a “bare” iron metal surface. Zn–HDTMP forms thin anticorrosive films that have a similar morphology.

Structural differences alone cannot explain the various corrosion efficiencies observed with the present inhibitors in the presence of metal ions such as  $\text{Ca}^{2+}$  or  $\text{Zn}^{2+}$ . Other factors such as the solubility of the metal–phosphonate complex, complex formation ability (either in the bulk or on the metal surface), and protective film thickness and integrity certainly have a significant role. For example, the complex formation constant for Zn–AMP is 16.4 and that for Zn–PBTC is 8.3.<sup>20</sup> The observed more-effective corrosion protection of a Zn–AMP film (which has a corrosion rate of 0.90 mm/yr at pH 3.0), compared to the corrosion inhibition of a Zn–PBTC film (which has a corrosion rate of 1.17 mm/yr at pH 4.0), is consistent with the higher complex formation constant of the former. This point is further supported by the fact that corrosion protection by Zn–AMP is better, even at a lower pH (3.0), compared to that of Zn–PBTC at a higher pH value (4.0). Similar arguments can be made for HDTMP; however, unfortunately, complex formation data are not available for this phosphonate.<sup>20</sup> The complex formation constant for Zn–EDTMP (which is a tetraphosphonate similar to HDTMP, but with a two-carbon-chain, instead of six-carbon-chain, linker between the aminomethylenephosphonate groups) has been reported to be 19.2. It is reasonable to assume that a similar complex formation constant may be determined for Zn–HDTMP.

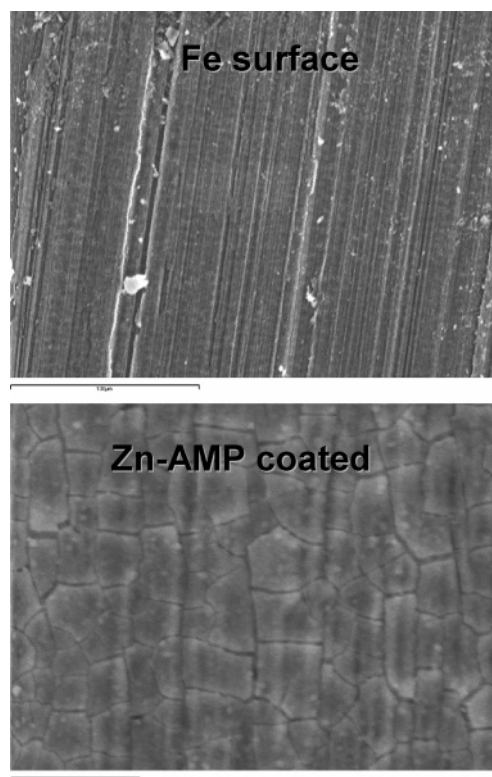


**Figure 9.** Scanning electron microscopy (SEM) images of a “clean” carbon steel surface (upper image, bar = 100  $\mu\text{m}$ ) and a Zn–AMP-protected steel surface (lower image, bar = 10  $\mu\text{m}$ ). The deposition of an anticorrosive Zn–AMP thin film is obvious. Film cracking is due to drying.

## Conclusions/Perspectives

The overall demand for corrosion inhibitors has been forecast to increase 4.4% per year, reaching \$1.6 billion in 2006, in the United States.<sup>26</sup> The petroleum refining sector is expected to have an approximately \$400 million share in this value. Corrosion is an economical burden for several industry sectors. Research on the subject has been active for several decades. The solution to this complicated issue requires a multidisciplinary approach that unifies researchers from a diverse list of scientific and technological disciplines: chemistry, chemical engineering, electrochemistry, materials science and engineering, and many others. Our contribution to advancing solutions for corrosion issues relevant to industrial problems lies with the study of the corrosion event and its inhibition *at the molecular level*. In this context, we have shown that a conveniently synthesized and structurally characterized Zn–AMP organic–inorganic hybrid polymeric material can act as a protective corrosion inhibitor by drastically reducing corrosion rates from 2.5 mm/yr (control) to 0.9 mm/yr (Zn–AMP protected sample). Furthermore, a Zn–HDTMP material can also protect carbon steel surfaces by reducing the corrosion from 7.28 mm/yr (for the control) to 2.11 mm/yr (for the Zn–HDTMP protected sample). In contrast, M–PBTC materials (where M = Ca, Zn) are ineffective corrosion inhibitors and, in fact, enhance corrosion rates from 0.16 mm/yr (for the control) to 1.17 mm/yr (for the Ca–PBTC protected sample) and 0.46 mm/yr (for the Zn–PBTC protected sample).

This paper is part of our ongoing effort on the issue of phosphonate-mediated corrosion protection. Understanding the intricate mechanisms of materials failure and its mitigation will enable us to improve current practices and invent novel ways to inhibit corrosion.

## Acknowledgment

The authors thank the following entities: the Department of Chemistry, University of Crete for financial support; Solutia—Europe for samples of AMP, HDTMP, and PBTC; and the research group of P. G. Koutsoukos at the University of Patras for experimental help.

## Literature Cited

- (1) Droffelaar, H.; Atkinson, J. T. N. *Corrosion and Its Control*; National Association of Corrosion Engineers (NACE) International: Houston, TX, 1995.
- (2) Javaherdashti, R. *Anti-Corros. Methods Mater.* **2000**, 47 (1), 30.
- (3) Gunasekaran, G.; Natarajan, R.; Muralidharan, V. S.; Palaniswamy, N.; Appa Rao, B. V. *Anti-Corros. Methods Mater.* **1997**, 44 (4), 248.
- (4) Palaniswamy, N.; Natarajan, R.; Appa Rao, B. V. *Anti-Corros. Methods Mater.* **1999**, 46 (1), 23.
- (5) Demadis, K. D.; Katarachia, S. D.; Koutmos, M. *Inorg. Chem. Commun.* **2005**, 8, 254.
- (6) Demadis, K. D.; Mantzaridis, C.; Raptis, R. G.; Mezei, G. *Inorg. Chem.* **2005**, 44, 4469.
- (7) Demadis, K. D.; Lykoudis, P.; Raptis, R. G.; Mezei, G. *Cryst. Growth Des.* **2006**, 6, 1064.
- (8) NACE Standard TM0169-95 (Item No. 21200), National Association of Corrosion Engineers (NACE) International, Houston, TX.
- (9) Gomez-Alcantara, M.; Cabeza, A.; Martinez-Lara, M.; Aranda, M. A. G.; Suau, R.; Bhuvanesh, N.; Clearfield, A. *Inorg. Chem.* **2004**, 43, 5283.
- (10) Song, H.-H.; Zheng, L.-M.; Wang, Z.; Yan, C.-H.; Xin, X.-Q. *Inorg. Chem.* **2001**, 40, 5024.
- (11) Drumel, S.; Janvier, P.; Deniaud, D.; Bujoli, B. *J. Chem. Soc., Chem. Commun.* **1995**, 1051.
- (12) Hartman, S. J.; Todorov, E.; Cruz, C.; Sevov, S. C. *Chem. Commun.* **2000**, 1213.
- (13) Mao, J.-G.; Clearfield, A. *Inorg. Chem.* **2002**, 41, 2319.
- (14) Yang, B.-P.; Mao, J.-G.; Sun, Y.-Q.; Zhao, H.-H.; Clearfield, A. *Eur. J. Inorg. Chem.* **2003**, 4211.
- (15) Demadis, K. D.; Sallis, J. D.; Raptis, R. G.; Baran, P. *J. Am. Chem. Soc.* **2001**, 123, 10129.
- (16) Kato, Y.; Toledo, L. M.; Rebek, J., Jr. *J. Am. Chem. Soc.* **1996**, 118, 8575.
- (17) Kalman, E.; Lukovits, I.; Palinkas, G. *ACH—Mod. Chem.* **1995**, 132, 527.
- (18) Bofardi, B. P. In *Reviews on Corrosion Inhibitor Science and Technology*; Raman, A., Labine, P., Eds.; National Association of Corrosion Engineers (NACE) International: Houston, TX, 1993; p II-6.
- (19) Sastri, V. S. *Corrosion Inhibitors: Principles and Applications*; Wiley: Chichester, U.K., 1998; p 720.
- (20) Knepper, T. P. *Trends Anal. Chem.* **2003**, 22, 708.
- (21) Demadis, K. D.; Katarachia, S. D. *Phosphorus Sulfur Silicon Relat. Elem.* **2004**, 179, 627.
- (22) Rajendran, S.; Appa Rao, B. V.; Palaniswamy, N. *Anti-Corros. Methods Mater.* **1998**, 45 (5), 338.
- (23) Gunasekaran, G.; Palanisamy, N.; Appa Rao, B. V.; Muralidharan, V. S. *Electrochim. Acta* **1997**, 42, 1427.
- (24) Kalman, E.; Karman, F. H.; Telegdi, J.; Varhegyi, B.; Balla, J.; Kiss, T. *Corros. Sci.* **1993**, 35, 1477.
- (25) Kuznetsov, Y. I.; Kazanskaya, G. Y.; Tsiurlikova, N. V. *Prot. Met.* **2003**, 39, 120.
- (26) Editorial. *Chem. Process.* **2002**, (December), 11.B.

Received for review June 21, 2006

Revised manuscript received September 15, 2006

Accepted September 16, 2006

IE0607898